Research Article

Received: 17 July 2025 Revised: 7 April 2026 Published online in Wiley Online Library: 19 May 2026

(wileyonlinelibrary.com) DOI 10.1002/jctb.70190

The use of activated carbon derived from spent coffee grounds as a reusable, sustainable, and effective solution for the removal of butylparaben from water

Lorena Maihury Santos Tsubouchi,[a] Diane Scapin,[b] Gideã Taques Tractz,[c] Flávia Aparecida Reitz Cardoso,[d,e] Lúcio Cardozo-Filho,[f] Alessandro Francisco Martins,[g] Diógenes Vedoy,[h] Ana Paula Peron[b,d,e] and Osvaldo Valarini Junior[d,e*]

Abstract

BACKGROUND: Parabens, including butylparaben (BP), are widely used as antimicrobial preservatives in food, cosmetics, and pharmaceuticals, yet are poorly removed by conventional water treatment processes and pose potential risks to aquatic life and human health. This study evaluates activated carbon produced from coffee grounds and chemically activated with $ZnCl_2$ ($ACZnCl_2$, 564.4 $m^2 \cdot g^{-1}$) as a sustainable adsorbent for BP removal from water.

RESULTS: Using 5 $g \cdot L^{-1}$ of $ACZnCl_2$ at pH 7, the highest removal efficiency (77.6 ± 0.4%) occurred at the lowest BP concentration (30 $\mu g \cdot L^{-1}$), with removal efficiency dropping to 20.0 ± 0.6% when BP concentration increases to 300 $\mu g \cdot L^{-1}$. While most studies examine high BP concentrations (10–200 $mg \cdot L^{-1}$), this work demonstrates effective removal at environmentally relevant trace levels. Equilibrium was reached within 100 min, and adsorption kinetics behavior were well described by PFO and PSO models ($R^2 = 0.998$). Equilibrium data fit the Langmuir isotherm ($R^2 = 0.996$), indicating monolayer adsorption. Thermodynamic parameters confirmed a spontaneous ($\Delta G \leq 0$) and exothermic ($\Delta H \leq 0$) adsorption process. Aspen Adsorption® simulations validated the system, predicting 100% theoretical removal. $ACZnCl_2$ maintained removal efficiency above 92% after six ethanol regeneration cycles. *Allium cepa* assays confirmed the elimination of cytotoxicity and genotoxicity in treated effluent.

CONCLUSION: The study shows that a 0.001 m-high adsorption column can treat water containing 600 $\mu g \cdot L^{-1}$ BP at a flow rate of 5×10^{-7} $m^3 \cdot s^{-1}$, highlighting $ACZnCl_2$ as a sustainable and scalable option with strong potential for practical water-treatment applications.

* *Correspondence to: OV Junior, Postgraduate Program in Technological Innovations. Federal Technological University of Paraná. Campo Mourão, Paraná, Brazil, E-mail: osvaldovalarini@utfpr.edu.br (Junior)*

a *Academic Department of Food and Chemical Engineering (DAAEQ), Federal Technological University of Paraná, Campo Mourão, Brazil*

b *Graduate Program in Environmental Engineering (PPGEA), Federal Technological University of Paraná, Francisco Beltrão, Brazil*

c *Academic Department of Chemistry (DAQUI), Federal University of Technology of Paraná, Campo Mourão, Brazil*

d *Postgraduate Program in Technological Innovations, Federal Technological University of Paraná, Campo Mourão, Brazil*

e *Postgraduate Program in Food Technology (PPGTA), Federal Technological University of Paraná, Campo Mourão, Brazil*

f *Department of Chemical Engineering, State University of Maringa, Maringa, Brazil*

g *Department of Chemistry, Heckert-Wells Hall, Office 105G, National Institute for Materials Advancement (NIMA), Pittsburg State University, Pittsburg, KS, USA*

h *Canadian Conservation Institute (CCI), Ottawa, Canada*

© 2026 The Author(s). *Journal of Chemical Technology and Biotechnology* published by John Wiley & Sons Ltd on behalf of Society of Chemical Industry (SCI).

This is an open access article under the terms of the Creative Commons Attribution License, which permits use, distribution and reproduction in any medium, provided the original work is properly cited.

© 2026 The Author(s). *Journal of Chemical Technology and Biotechnology* published by John Wiley & Sons Ltd on behalf of Society of Chemical Industry (SCI).

Supporting information may be found in the online version of this article.

Keywords: equilibrium isotherms; Gibbs free energy; non-toxicity; paraben; simulation Aspen; zinc chloride

INTRODUCTION

BP (butylparaben) is a carboxylic acid–based compound widely used as an active ingredient in pharmaceuticals, cosmetics, and processed foods.[1] As a result of its widespread use, BP contaminates water and soil.[2]

Paraben compounds, including BP, are potentially toxic and are not effectively removed by standard water treatment methods.[2] Although these compounds degrade in about ten days in water and soil, their continuous release leads to widespread accumulation and environmental toxicity.[1-4] BP is known to disrupt neurotransmitter systems and cause renal and cranial issues in fish, even at small concentrations, *i.e.*, microgram-per-liter.[1,5,6] In humans, BP is associated with infertility and neoplasms development in women.[4,7]

Unconventional methods for treating emerging pollutants like BP include oxidative processes, ion exchange, membrane separation, and electroprecipitation.[8] However, these methods often generate waste and require intensive equipment maintenance. Adsorption is an alternative treatment with advantages such as lower costs and adaptability to specific treatment needs.[9] Adsorption treatments generally exhibit high pollutant removal efficiency and allow for the reuse of discarded materials as precursors for the production of activated carbon (AC), reducing environmental impact.[10]

Carbonaceous materials have high potential for use in adsorption treatments because they can be produced on an industrial scale.[11] After calcination, they are transformed into AC, a functional material with a porous and crystalline structure. The porosity and adsorption efficiency of AC structure can be further enhanced using chemical, physical, or biological activating agents.[8]

ACs are widely used in water and gas treatment due to their strong interaction with organic pollutants. ACs materials are classified by particle size as powders, pellets, or granules.[12] ACs pores range from micropores to macropores, with their proportion influenced by activation methods and operational conditions.[13] In adsorption systems, ACs interact with compounds such as oxygen, hydrogen, and nitrogen, forming various functional groups, including carboxylic acids, hydroxyls, lactone carbonyls, and quinones.[14,15]

Spent coffee grounds (SPG) from *Coffea arabica L*. are a promising precursor material for the production of AC in large scale since approximately two billion tons of SPG are generated annually from the consumption of coffee, which reached 50.3 million (50 kg-bags) in global production in 2022.[16] If simply discarded in the environment, SPGs poses environmental challenges; in aquatic environments, SPGs resist decomposition due to the presence of caffeine, fatty acids, and metals, while in landfills, SPGs can produce difficult-to-treat leachate.

SPG consists of approximately 50% carbon, 49% lignin, and minor amounts of hydrogen and nitrogen. During carbonization, hydrogen and oxygen are released from the material. Due to the high toxicity of SPG sludge, which makes environmental treatment difficult, carbonization is a promising method for repurposing this waste.[13] Calcining SPG in an inert nitrogen atmosphere produces AC with a porous surface ideal for adsorption. Optimizing the temperature for low ash production, removing volatile compounds, and using chemical agents to enhance pore formation all contribute to a high AC yield. These qualities, combined with the sustainable production, make AC derived from SPG an attractive option for commercial use.[8,17,18]

Several studies have used computational tools and laboratory tests to evaluate the adsorption dynamics in fixed-bed columns. Yasir *et al.*,[19] modeled the removal of 2,4-dichlorophenol using Aspen Adsorption®, comparing the performance of activated carbon with low-cost residues, such as bagasse ash and rice husk ash. The results showed optimal performance in beds taller than 3 m and flow rates below 5.56×10^{-6} $m^3 \cdot s^{-1}$, with rice husk ash showing the highest adsorptive capacity among those tested.[20] Similarly, Soriano *et al.*[21] investigated heavy-metal biosorption and observed that the breakthrough time is inversely proportional to the input concentration. At loads of 50 ppm, saturation occurred more rapidly, demonstrating that higher concentration gradients accelerate mass transfer in the system.

Recently, the herbicide/adsorbent interactions that underlie this work were experimentally analyzed by Moraes *et al.*[22] and Rocha *et al.*[8] Although they operated with concentrations lower than those reported here, the authors recorded removal efficiencies of 100% for diuron, 70% for bentazone, and 45% for linuron after 24 h. In these studies, the kinetic behavior was adequately described by the first-order model, while the adsorption equilibrium followed the Langmuir model.

This study presents a novel adsorption system using activated carbon produced with coffee grounds and activated with $ZnCl_2$ ($ACZnCl_2$) for the efficient and environmentally friendly removal of BP. Dynamic simulations validate laboratory experiments by modeling adsorption columns with mass conservation, kinetic, and equilibrium equations, as implemented in the Aspen Adsorption® software. Notably, pharmaceutical product simulations using Aspen Adsorption® have not previously been reported.[23-25]

The research objectives included:

(1) Evaluating removal efficiency;
(2) Predicting system behavior *via* computational modeling;
(3) Assessing kinetic models (PFO, PSO, EL, ID);
(4) Investigating ionic and temperature effects;
(5) Studying Langmuir and Freundlich isotherms;
(6) Assessing adsorbent reusability; and
(7) Performing toxicological analyses on treated and untreated effluents.

This approach highlights the innovative use of waste-derived adsorbents and advanced modeling to promote sustainable water treatment solutions.

EXPERIMENTAL

The reagents used were SPG (provided by the company Coamo), $ZnCl_2$, and BP (all analytical grade). The adsorption experiments were conducted using a Tecnal Shaker TE-4200 and a Global Analyzer UV–VIS spectrophotometer, both acquired in São Paulo, Brazil.

Preparation and characterization of activated carbon ($ACZnCl_2$)

$ACZnCl_2$ was synthesized from SPG, a carbon-rich and lignocellulosic waste material, using chemical activation with $ZnCl_2$. SPG and $ZnCl_2$ were mixed in a 2:1 mass ratio under continuous agitation at 50 rpm and heated to 85 °C for 7 h. The mixture was then subjected to further thermal treatment at 110 °C for 24 h. After cooling to room temperature, the dried material was calcined at 600 °C for 2 h under a nitrogen atmosphere (1 mL·min^{-1} flow rate) in a muffle furnace.

Post-calcination, the carbonized material was washed with 0.1 M hydrochloric acid for 20 min at 25 °C to remove residual activating agents and impurities. The final product was sieved to obtain a uniform particle size of 100 mesh.

This functionalized carbon material, previously reported by Moraes *et al.*[22] and Rocha *et al.*,[8] exhibited high performance in adsorption applications, achieving a removal efficiency of 97.2%. Characterization revealed an ash content of 1.95 ± 0.07%, volatile matter of 3.38 ± 1.98%, and a pH of 5.8. Textural analysis (*e.g.*, specific surface area, total pore volume, *etc.*) is presented in Table 1.

Adsorption tests

All adsorption experiments were conducted at controlled temperatures and agitation speeds.

Solution preparation

NaOH and HCl stock solutions (0.1 M) were prepared by weighing one-tenth of their molar mass using a Mettler Toledo (Brazil) analytical balance, then dissolving each in 1 L of ultrapure water. These solutions were used to control and adjust pH as needed.

A stock solution of butylparaben (BP, 600 μg·L^{-1}) was prepared in ultrapure water and used in all adsorption experiments.

Working solutions for removal efficiency tests were prepared by diluting the BP stock with ultrapure water to obtain final BP concentrations of 30, 300, and 600 μg·L^{-1}.[26,27] The selection of trace-level concentrations (30–600 μg·L^{-1}) reflects environmental conditions, as parabens are typically detected in rivers at μg·L^{-1} levels.[19,28] All solutions were prepared in triplicate. Equipment was calibrated using blanks (without BP) to avoid interference during measurements.

Table 1. Physicochemical parameters of $ACZnCl_2$[8]

Description	$ACZnCl_2$
BET surface area ($m^2.g^{-1}$)	564.366
Micropore area ($m^2.g^{-1}$)	501.959
External surface area ($m^2.g^{-1}$)	66.407
Average pore diameter (nm)	1.116
Micropore volume ($cm^3.g^{-1}$)	0.256
Boehm method Carboxylics (mmol.g^{-1})	0.0794
Boehm method Lactonics m_{eq} (mmol.g^{-1})	0.0021
Boehm method Phenolics m_{eq} (mmol.g^{-1})	0.0182
Stretching bond groups -N-H and -OH	1377 cm^{-1}
-C-OH stretching - FTIR	1088 cm^{-1},
-C-N stretching – FTIR	613 cm^{-1}
-C-O-C vibrations – FTIR	1165 cm^{-1}
O-H stretching vibrations	3400 cm^{-1}

Kinetics and equilibrium adsorption

- Kinetic studies were conducted under conditions that yielded the highest removal efficiency (*ER%*), which was calculated using Eqn (S1).
- The adsorption of BP was monitored over time intervals ranging from 0 to 1440 min.
- Experimental data on adsorption kinetics (Q_e) were determined using Eqn (S2). The kinetic models are shown in Eqns (S3–S6). Experimental data were fitted to several kinetic models: pseudo-first order (PFO), pseudo-second order (PSO), Elovich (EL), and intraparticle diffusion (ID) models, to characterize the adsorption mechanism.[8,22,29]
- Equilibrium isotherms were obtained for BP concentrations between 0 and 55 μg·L^{-1}, under the same temperature, agitation, and contact time used in the adsorption kinetic experiments. UV–Vis absorbance values were converted into equilibrium concentrations (C_e) and adsorption capacities (Q_e). After equilibrium time was reached, samples were filtered, and the residual BP concentration was quantified. Q_e was then plotted as a function of C_{eq}, and the Langmuir Eqn (S7), Freundlich Eqn (S8), Temkin Isotherm Eqn (S9), and Dubinin-Radushkevich Isotherm Eqn (S10) models were fitted to the experimental equilibrium data.

Thermal and ionic tests, regeneration protocol, and toxicity test

Ionic strength tests

The effect of ionic strength was assessed by adding varying concentrations of sodium chloride (NaCl) to the BP solution with activated carbon. Three NaCl concentrations were tested to evaluate the role of electrostatic interactions.[30]

Temperature effect

Experiments were conducted at three temperatures to examine the effect of temperature on adsorption capacity and thermodynamic parameters, specifically enthalpy, entropy, and Gibbs free energy. The same experimental setup as the isotherm tests was used, and thermodynamic values were reported in kJ·mol^{-1}·K^{-1} units.[30] $\Delta G°$ is defined according to Eqn (S11). $\Delta G°$ is the equilibrium constant K_{eq} (L·mol^{-1}), according to Eqn (S12). Correlating equations, we obtain the relationship between K_{eq}, $\Delta H°$, and $\Delta S°$, as shown in Eqn (S13).

Regeneration and reuse protocol

The reuse of $ACZnCl_2$ was tested following its use in BP removal. After each adsorption cycle, the spent adsorbent was centrifuged with 99.5% ethanol for 5 h to desorb BP, followed by washing with deionized water to remove residual solvent and restore pH. After drying to constant humidity, the $ACZnCl_2$ was reused in up to six consecutive adsorption cycles.[31,32]

Toxicity testing

Toxicity was assessed using cytotoxicity and genotoxicity tests, according to methodologies established by Fiskesjö.[33] Both tests were performed in aqueous solutions, with and without the adsorbent.

J Chem Technol Biotechnol 2026; **101**: 1547–1558 © 2026 The Author(s). wileyonlinelibrary.com/jctb
Journal of Chemical Technology and Biotechnology published by John Wiley & Sons Ltd on behalf of Society of Chemical Industry (SCI).

- The onion (*Allium cepa*) root assay was used to evaluate toxicity: bulbs were exposed to BP-contaminated solutions for five days.
- Controls included BP concentrations of 30 and 600 $\mu g \cdot L^{-1}$, and deionized water (as a negative control).
- Post-exposure, roots were fixed in Carnoy's solution (3:1 v:v) for 24 h, then hydrolyzed. Meristem tissues were prepared on slides for microscopic observation (400× magnification).
- Cytotoxicity was quantified using the Mitotic Index (*MI*), as described in Eqn (S14), by counting 2000 cells per onion (10 000 cells per treatment).
- Genotoxicity was determined using the Cell Alteration Index (*CAI*), as given in Eqn (S15), by analyzing chromosomal aberrations in 200 cells per onion (1000 cells per treatment).

Statistical analysis

Results from all tests were compared using Kruskal–Wallis ANOVA to identify significant differences ($P \leq 0.05$), followed by Dunn's *post hoc* test. All statistical analyses were conducted using RStudio (free version).

SIMULATION

The simulation workflow followed the steps outlined in Fig. S1. The theoretical framework for simulating BP adsorption onto $ACZnCl_2$ was implemented using Aspen Adsorption® V14.1.

The simulation relied on key process parameters. Since the molecular dimensions of BP are smaller than the pore sizes of $ACZnCl_2$, Knudsen diffusion was considered. Flow through the adsorption bed was assumed to occur strictly in the axial direction, with a constant cross-sectional area along the entire bed length. The system was simulated under isothermal conditions, maintaining constant pressure and linear velocity throughout.

The adsorbent particles were modeled as spherical and homogeneous in both size and density.[25] For fixed-bed modeling, a first-order Upwind discretization scheme was used.

Mass/momentum balance

In this study, the mass/momentum balance was considered under convective transport with estimated dispersion. The partial mass balance for the concentration of parabens within a differential volume element of the adsorption column is represented by the following partial differential equation [Eqn (S16)]:

Equation (S16) encompasses several phenomena: the axial dispersion, represented by the first term; convective mass transfer, the second term, which signifies the accumulation of pollutants in adsorbents; and the third term, representing the adsorption of BP onto adsorbent particles. D_z is the axial dispersion coefficient ($m^2 \cdot s^{-1}$), q is the concentration of parabens adsorbed in the solid phase ($mg \cdot g^{-1}$), C is the concentration in the liquid phase ($mg \cdot L^{-1}$), z is the distance along the bed (m), v_i is the interstitial velocity of the fluid through the bed ($m \cdot s^{-1}$). ϵ is the bed void fraction (dimensionless) and ρ_b is the bulk density of the bed ($kg \cdot m^{-3}$). D_z was estimated using Eqn (S17).[21] Where, d_p is the adsorbent particle diameter given in meters (m), and Re is the Reynolds number, used to determine if the system is laminar or turbulent.

Kinetic model

The kinetic model employed in this study was the lumped linear resistance model (PFO-experimental) [Eqn (S3)], which is a first-order model. This model indicates that the mass transfer coefficient (K_i) occurs in the solid phase and is expressed in s^{-1}. The variable Q_e is defined as the instantaneous equilibrium concentration ($\mu g \cdot g^{-1}$). If we consider both external fluid film resistance and pore diffusional resistance, K_i can be estimated using Eqn (S18).

Where k_{fi} is the external film mass transfer coefficient of adsorbate i ($m \cdot s^{-1}$), and D_p is the effective pore diffusivity coefficient ($m^2 \cdot s^{-1}$). The missing parameters k_{fi}, D_p, the Knudsen diffusion coefficient (D_k) ($m^2 \cdot s^{-1}$), and the molecular diffusion coefficient of $ACZnCl_2$ (D_m) ($m^2 \cdot s^{-1}$) were estimated using empirical correlations. The data from Table S1 were used to determine the parameters reported in the previous equations.

Adsorption isotherm

The equilibrium isotherm used for the $ACZnCl_2$ adsorption process with BP was the Langmuir model, which has been validated in numerous studies by the group.[8,11] The Langmuir model is represented by Eqn (S7), but in Aspen Adsorption®, the Langmuir isotherm is expressed by Eqn (S19).[25]

In these equations, Q_e and w_i represent the amount of solute removed per unit mass of adsorbent, given in $\mu g \cdot g^{-1}$ and $kmol \cdot kg^{-1}$, respectively. Q_{max} and IP_1 correspond to the maximum solid-phase adsorption in the monolayer, with units identical to those of Q_e and w_i; k_L and IP_2 are the energy constants related to the heat of adsorption, with units of $L \cdot \mu g^{-1}$ and $m^3 \cdot kmol^{-1}$, respectively. The quantitative values for IP_1 and IP_2 can be obtained from Eqns (S20-S21).

Where M is defined as the molecular mass of the parabens ($g \cdot mol^{-1}$). The bed height (H_b) is fixed in meters. In the product section, the flow rate, temperature, and pressure remain constant, matching the inlet values of the adsorption process.

Column performance study

The performance of the adsorption process for BP was evaluated based on breakthrough time (t_{Break}, sec), volumetric flow rate (Q, $m^3 \cdot s^{-1}$), saturation time (t_{Sat}, sec), and the total volume of treated solution (V_{eff}, m^3), as estimated using Eqns (S22–S24). The analysis was performed over the concentration range of 0.05 to 0.9 in terms of the normalized concentration ratio ($C \cdot C_i^{-1}$), where C_R represents the concentration of BP in the effluent ($mg \cdot L^{-1}$), and m denotes the mass of the adsorbent (g) packed in the fixed-bed column.

EXPERIMENTAL RESULTS AND DISCUSSION

Adsorption test - experimental

To determine the removal efficiency (*ER%*), a mixture comprising 50 mL of BP solution and 5 $g \cdot L^{-1}$ of $ACZnCl_2$ was prepared at pH 7. The mixture was agitated at 50 rpm and maintained at room temperature for 24 h. After 24 h, the final BP concentration (C_{Final}) was determined by measuring UV–Vis absorbance at 254 nm. The absorbance values were converted to concentration using the linear calibration curve,[34] see Eqn (S1).

The removal efficiency (*ER%*) values obtained were:

- 77.6 ± 0.4% for 30 $\mu g \cdot L^{-1}$ BP,
- 20.0 ± 0.6% for 300 $\mu g \cdot L^{-1}$ BP, and
- 22.4 ± 0.8% for other tested concentrations.

The highest removal efficiency was observed at 30 $\mu g \cdot L^{-1}$. This result can be explained by lower competition for adsorption sites at lower BP concentrations, allowing more BP molecules to be trapped within the $ACZnCl_2$ microporous structure.[8] This adsorption is further facilitated by the large surface area of $ACZnCl_2$

© 2026 The Author(s).

Journal of Chemical Technology and Biotechnology published by John Wiley & Sons Ltd on behalf of Society of Chemical Industry (SCI).

(564.37 $m^2 \cdot g^{-1}$) and the relatively small size of the BP molecule (molar mass: 194.23 $g \cdot mol^{-1}$).

The chemical properties of AC, such as specific functional groups, along with other physical–chemical factors, greatly influence removal efficiency. In this study, we were interested in the contribution of AC chemical properties while holding constant variables such as polarity, ionic strength, and pH.[35,36] To put the findings presented above in perspective, da Rocha *et al.*[8] reported an *ER%* of 74% using commercial activated carbon for octocrylene removal at 30 $\mu g \cdot L^{-1}$ octocrylene and 5 $g \cdot L^{-1}$ adsorbent. Under similar conditions, $ACZnCl_2$ achieved an *ER%* of 82%. Other studies have reported *ER%* values of 69.67% at 50 mg/L bentazone using 10 $\mu g \cdot L^{-1}$ ACs and,[8] for $ACZnCl_2$, an *ER%* of 99.3% for diuron and 45.2% for linuron at 40 $\mu g \cdot L^{-1}$ and 31 $\mu g \cdot L^{-1}$, respectively.[22]

The enhanced performance of $ACZnCl_2$ can be attributed to chemical activation with $ZnCl_2$, which dehydrates lignocellulosic materials (such as spent coffee grounds), increases surface area and pore volume, and introduces additional functional groups (hydroxyl, carboxylic acid, carbonyl, lactone, and quinone) onto the carbon surface.[37-39] Compared to other common activators like KOH and H_3PO_4, $ZnCl_2$ offers superior activation properties.

Although the precise mechanisms of organic contaminant adsorption onto $ACZnCl_2$ are complex, current studies suggest that BP degradation plays an important role in the adsorption process, particularly *via* radical-mediated reactions.[8,11,40,41] Chloride (Cl^-) and hydroxyl (OH^-) radicals formed during these reactions facilitate the adsorption and breakdown of BP, primarily through interactions between the pollutant's aromatic ring and hydroxyl groups on the adsorbent surface. In aqueous solutions, the transfer of π electrons and redox reactions on the $ZnCl_2$-functionalized surface further enhance BP removal efficiency.

Table 2. Kinetic and equilibrium isotherms values obtained using the experimental data related to the adsorption of the BP on $ACZnCl_2$

Kinetic	Calculated values and constants	
PFO	Q_e ($\mu g \cdot g^{-1}$)	1174.88 ± 8.38
	k_1 (min^{-1})	$1.36.10^{18}$ ± 0.001
	R^2	0.998
PSO	Q_e ($\mu g \cdot g^{-1}$)	1174.88 ± 4.92
	k_2 ($\mu g \cdot g^{-1} \cdot min^{-1}$)	$2.40.10^{13}$ ± 0.01
	R^2	0.998
EL	α ($\mu g \cdot g^{-1} \cdot min^{-1}$)	1.23 ± 0.23
	β ($\mu g \cdot g^{-1}$)	$-7.20.10^{46}$ ± 0.21
	R^2	—
ID	C ($\mu g \cdot g^{-1}$)	15.26 ± 0.65
	k_{di} ($min^{-0.5}$)	733.78 ± 0.73
	R^2	0.270
Isotherms	**Calculated values and constants**	
Langmuir	Qmax ($\mu g \cdot g^{-1}$)	5408.09 ± 17.04
	K ($L \cdot g^{-1}$)	0.005 ± 0.001
	R^2	0.996
Freundlich	K_f ($\mu g \cdot g^{-1} \cdot L^{-1/n}$)	2.57 ± 0.82
	n	0.95 ± 0.08
	R^2	0.984
Temkin	A_T	0.709 ± 0.371
	b_T	11.751 ± 1.99
	R^2	0.858
Dubinin-Radushkevich	Q_S	1116.955 ± 73.833
	k_{AD}	0.369 ± 0.091
	R^2	0.966

Kinetics and equilibrium adsorption

Kinetic model evaluation

Experimental adsorption kinetics (*e.g.*, Q_e) were determined using Eqn (S2). The kinetic models described by Eqns (S3–S6) correspond to the PSO, EL, and ID models. The PFO model, although not explicitly listed among these equations, was also included in the computational model.

Each model includes characteristic constants:

- Q_t: Total adsorption capacity ($\mu g \cdot g^{-1}$).
- k_1: PFO rate constant (min^{-1}).
- k_2: PSO rate constant ($\mu g \cdot mg^{-1} \cdot min^{-1}$).
- k_{id}: ID rate constant ($\mu g \cdot mg^{-1} \cdot h^{-0.5}$).
- α, β: Initial adsorption and desorption rate constants.

The adsorption capacity (Q_e) is calculated from the solution volume, adsorbent mass, and equilibrium concentration (C_e), with units of liters (L), grams (g), and $\mu g \cdot L^{-1}$, respectively. Concentration and adsorption capacity are ultimately expressed in $\mu g \cdot g^{-1}$.

Interpretation of kinetic models

Among the applied models:

- PFO model describes the adsorption driven by the initial concentration C_o.[42]
- PSO model assumes chemisorption, with the adsorption rate controlled by the availability of active sites rather than C_0.[43]
- EL model provides a better description of chemisorption on heterogeneous surfaces,[44] while the ID model accounts for diffusion within porous materials, describing the BP adsorption within $ACZnCl_2$ pores *via* interactions between aromatic ring ions and surface functional groups.[45] The mass transfer mechanism of the system is characterized by multilinear behavior, indicating that intraparticle diffusion within the pores is not the sole rate-limiting step. The deviation of the regression line from the origin suggests that boundary-layer (film) diffusion occurs simultaneously with internal transport. This confirms that while the high porosity of the SPG-derived carbon facilitates the internal movement of the adsorbate, initial external resistance still plays a significant role in the overall adsorption kinetics.[8,9,45,46]

The adsorption–desorption process reached equilibrium after approximately 100 min. Prior to this point, adsorption increased exponentially due to the abundance of unsaturated $ACZnCl_2$ pores. Upon pore saturation, a constant adsorption rate was achieved, and further uptake occurred through slower surface diffusion from solution to the carbon matrix.[9]

Table 2 presents calculated kinetic and equilibrium values alongside experimental data. The PFO and PSO models showed strong correlations ($R^2 = 0.998$), whereas the ID ($R^2 = 0.27$) and EL model did not correlate significantly with the experimental results.[43]

Isotherm models and adsorption behavior

Adsorption isotherms describe the equilibrium behavior of adsorbates in liquid–solid systems. According to IUPAC, six types of isotherms exist, categorized originally by Brunauer, Deming, Deming, and Teller (BDDT) in 1940.[47] In this study, four isotherm models were applied to evaluate the interaction between BP and $ACZnCl_2$:

J Chem Technol Biotechnol 2026; **101**: 1547–1558 © 2026 The Author(s). wileyonlinelibrary.com/jctb
Journal of Chemical Technology and Biotechnology published by John Wiley & Sons Ltd on behalf of Society of Chemical Industry (SCI).

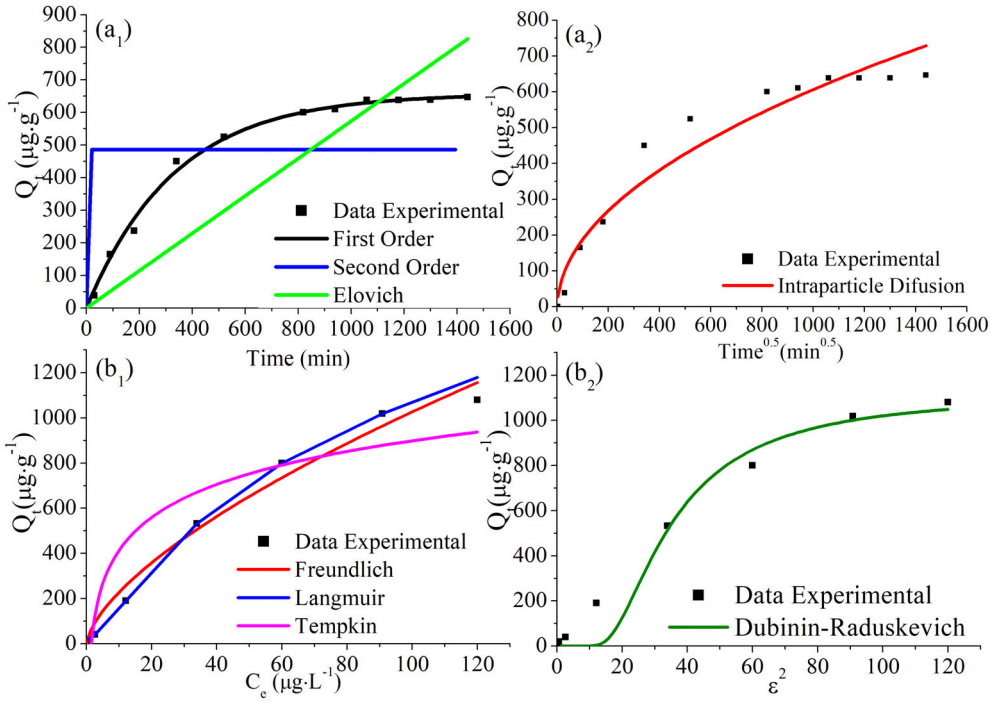


Figure 1. Kinetic models simulated from experimental data.

Langmuir Isotherm (Eqn S7): Describes monolayer adsorption on a homogeneous surface, where each site holds a single molecule without interactions between adsorbed molecules. It is highly suitable for chemical adsorption processes.[48]

Freundlich Isotherm (Eqn S8): An empirical model for multilayer adsorption on heterogeneous surfaces, assuming varying adsorption energies across sites, where surface heterogeneity is represented by the parameter n.[9] In the Freundlich model, the parameter $n > 0$ indicates that BP molecules adsorb spontaneously *via* mass transfer and electrostatic interactions.[8,11,43] Understanding these values helps elucidate adsorption mechanisms at the solid–liquid interface.

Temkin Isotherm (Eqn S9): Considers the effects of indirect adsorbate-adsorbate interactions, suggesting that the heat of adsorption decreases linearly with surface coverage.[49]

Dubinin-Radushkevich Isotherm (Eqn S10): A general model used to distinguish between physical and chemical adsorption mechanisms on non-homogeneous surfaces.[50]

Figure 1(b_1), (b_2) illustrate the fit of these models to the experimental data. The calculated parameters in Table 1 indicate that the Langmuir model provided a superior fit ($R^2 = 0.996$) compared to the Freundlich ($R^2 = 0.984$), Dubinin-Radushkevich ($R^2 = 0.966$), and Temkin ($R^2 = 0.858$) models.

The excellent fit of the Langmuir model suggests that adsorption occurs on a homogeneous surface *via* monolayer formation. The maximum adsorption capacity (Q_{max}) was 5408.09 ± 17.04 μg·g^{-1}, supporting the presence of a high surface area and sufficient pore volume in the $ACZnCl_2$ matrix to sequester the pollutant. In the Freundlich model, the parameter $n = 0.95 \pm 0.08$ indicates that BP molecules adsorb spontaneously through mass transfer and electrostatic interactions.

The Dubinin-Radushkevich model yielded a theoretical saturation capacity (Q_s) of 1116.955 ± 73.833 μg·g^{-1}with a k_{AD} of 0.369 ± 0.091 mol^2·kJ^{-2}. Meanwhile, the Temkin constants $A_T = 0.709$ and $b_T = 11.751$ suggest moderate interaction energies during the process.

The mean free energy of adsorption (E), calculated as $E = (2K_{AD})^{-0.5}$, was approximately 1.16 kJ·mol^{-1}. Values of E below 8 kJ·mol^{-1} are characteristic of a physisorption mechanism, confirming that the interaction between butylparaben and $ACZnCl_2$ is governed by physical forces, such as Van der Waals interactions and π-π stacking, consistent with the spontaneous, exothermic nature of the process.[51,52]

Desorption begins when the active sites in $ACZnCl_2$ are saturated, at which point BP molecules detach and return to the solution due to the monolayer nature of the material.[53]

Compared to other studies in the literature, the Langmuir isotherm consistently provides the best fit for systems involving emerging pollutants and activated carbon materials.[3,54-56] Because of its thermodynamic consistency and representation of homogeneous surfaces, it is the most accurate model for this study's experimental data.[57]

Effects of temperature and ionic, and regeneration and toxicity

Effect of ionic strength

As shown in Fig. 2(a), 99% of BP exists in its anionic form across all tested NaCl concentrations. The Q_t of $ACZnCl_2$ remained nearly constant despite increasing salt concentrations. This behavior is attributed to enhanced electrostatic repulsion between negatively charged BP and the negatively charged $ACZnCl_2$ surface. As NaCl concentration increases, the solution's ionic strength intensifies these repulsive interactions, thereby decreasing adsorption efficiency. Although electrostatic attraction can enhance adsorption, strong repulsion—especially under high ionic strength—can reduce it, as previously described by Spaltro *et al.*[30]

 © 2026 The Author(s).
Journal of Chemical Technology and Biotechnology published by John Wiley & Sons Ltd on behalf of Society of Chemical Industry (SCI).

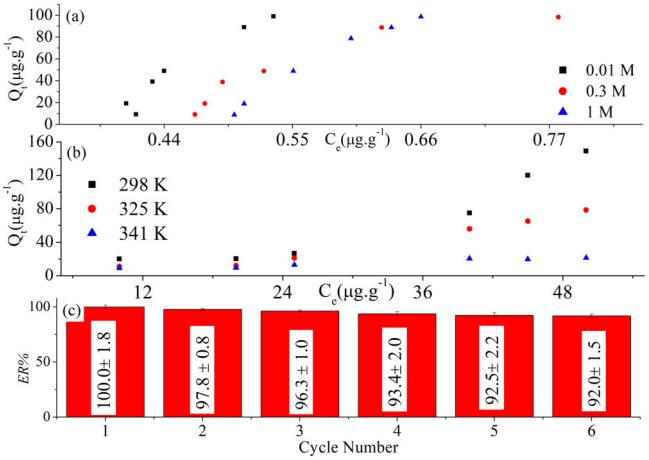


Figure 2. Equilibrium Isotherms (a) ionic and (b) temperature. (c) Regeneration cycles.

Effect of temperature and thermodynamic analysis

Figure 2(b) shows that total adsorption capacity decreases with increasing temperature, indicating that elevated temperatures are unfavorable for BP adsorption onto $ACZnCl_2$. This inverse relationship confirms the exothermic nature of the process, as adsorption is accompanied by energy release.[57,58]

Thermodynamic parameters were calculated using Eqns (S11–S13). The standard Gibbs free energy change ($\Delta G°$) was derived from the equilibrium constant (K_{eq}), and the relationships between $\Delta G°$, enthalpy ($\Delta H°$), and entropy ($\Delta S°$) were established using the van't Hoff equation. A linear plot of $\ln(K_{eq})$ *versus* $1/T$ was used to determine these parameters by least-squares fitting. This graphical analysis provides insights into the spontaneity of the process and heat exchange.

Table 3 presents the calculated values. The negative $\Delta G°$ values confirm the spontaneity of BP adsorption, while negative $\Delta H°$ values indicate that the process is exothermic. The positive $\Delta S°$ suggests increased randomness at the solid–liquid interface during adsorption.[30]

These findings are consistent with spontaneous, energetically favorable interactions.[13,55]

Toxicity reduction assessment

The toxicological impact of BP before and after adsorption was assessed using *Allium cepa*. Table 3 presents results for two concentrations: 30 and 600 $\mu g \cdot L^{-1}$. The mitotic index (*MI*) and chromosomal aberration index (*CAI*) were used to evaluate cytotoxic and genotoxic effects, respectively. Before treatment, BP significantly reduced cell division and increased chromosomal abnormalities. After passing through $ACZnCl_2$, BP-induced cytotoxicity and genotoxicity were no longer observed, demonstrating effective pollutant removal. These findings align with previous toxicological studies on BP in *Allium cepa* and human lymphocytes.[59,60]

Although additional trophic levels were not evaluated, the *Allium cepa* assay is widely recognized as a sensitive and reliable bioindicator of cytotoxicity and genotoxicity. The cellular mechanisms assessed—such as alterations in mitotic index and chromosomal aberrations—are highly conserved across eukaryotic organisms, allowing cautious extrapolation to other biological systems. Furthermore, previous studies have demonstrated good correlation between the *Allium cepa* assay responses and bioassays involving aquatic invertebrates and fish species.[58,61]

Table 3. Thermodynamic parameters for adsorption of the BP on $ACZnCl_2$ and toxicity values before and after adsorption using the Mitotic Index (MI) and the Cell Alteration Index (CAI)

Calculated thermodynamic data

T (K)	ΔH ($kJ \cdot mol^{-1}$)	ΔS ($kJ \cdot K^{-1} \cdot mol^{-1}$)	ΔG ($kJ \cdot mol^{-1}$)
293	−6.471	$3.55.10^{-3}$	−7.507
325	—	—	−7.620
341	—	—	−7.677

MI and CAI values for root meristems of *Allium cepa* L.

Adsorption run	BP concentration ($\mu g \cdot L^{-1}$)	MI/SD (%) 100.00 ± 0.8	ICC/SD (%) 0.1 ± 0.9
Before	30	59.1 ± 0.5*	17.4 ± 0.6*
	600	59.0 ± 0.8*	38.9 ± 0.9*
After	30	94.1 ± 0.9	0.3 ± 0.9
	600	90.9 ± 0.7	0.1 ± 0.7

Therefore, the observed reduction in cytogenotoxic effects following adsorption suggests a substantial decrease in the biological risk of the treated effluent.

Regeneration and reuse of $ACZnCl_2$

The reuse potential of $ACZnCl_2$ was evaluated across six regeneration cycles. Figure 2(c) shows that the adsorbent maintained high efficiency throughout, with only a slight decline after the fourth cycle. In the first three cycles, the BP removal efficiency (*ER%*) remained above 96%:

- Cycle 1: 100% *ER* (±1.8%).
- Cycle 2: 97% *ER* (±0.8%).
- Cycle 3: 96.3% *ER* (±1.0%).

After the third cycle, *ER%* slightly declined, likely due to saturation of active sites and minor thermal degradation during regeneration. Nevertheless, the material consistently maintained an efficiency of over 92%, confirming its high regeneration potential. These results are consistent with findings by Namasivayam and Sangeetha,[62] and Dąbek.[63]

Comparative adsorption performance

Compared to $ACZnCl_2$, other adsorbents demonstrate lower removal efficiencies. For example, graphene oxide achieved only ~20% BP removal under pH 6 and 400 $mg \cdot L^{-1}$ concentration.[12] Additionally, adsorbents made from African palm bark (*Elaeis guineensis*) activated with calcium and magnesium chloride also exhibited low removal efficiency. These systems, such as $ACZnCl_2$, showed negative ΔG and ΔH values—indicating spontaneous, exothermic processes—but their performance remained inferior.[14]

SIMULATION RESULTS AND DISCUSSION

The validation of the adsorption model was carried out using experimental data from previous work on bentazone removal by $ACZnCl_2$, as reported by Rocha *et al.*[8] The process configuration used for validation followed the model presented in Fig. 1. To reproduce the experimental conditions, the simulation employed a volumetric flow rate approaching zero, corresponding to the

J Chem Technol Biotechnol 2026; **101**: 1547–1558 © 2026 The Author(s). wileyonlinelibrary.com/jctb
Journal of Chemical Technology and Biotechnology published by John Wiley & Sons Ltd on behalf of Society of Chemical Industry (SCI).

Table 4. Physicochemical properties of the adsorbent and adsorbate estimated using Aspen Adsorption® for different paraben concentrations

Property	Value	References
Paraben Concentration ($\mu g \cdot L^{-1}$)	30–300-600	Variable
Water Concentration ($kmol \cdot m^{-3}$)	55.55	Fixed
Height of adsorbent layer (m) - H_b	0.001	Fixed
Particle radius (m) - R_P	8.47×10^{-8}	Fixed
Pore radius (m) - r_p	1.11×10^{-9}	Fixed
Diameter of adsorbent layer d_p (m)	1.69×10^{-7}	Fixed
Inter-particle voidage (m^3 void$\cdot m^{-3}$ bed^{-1}) - ε_b	0.50	Fixed
Particle porosity - ε_P	0.42	Fixed
Bulk Density ($kg \cdot m^3$) - ρ_{ACZnCl_2}	740	Fixed

Table 5. Parameters calculated and utilized for a volumetric flow rate of 12 000 $m^3 \cdot day^{-1}$ using $ACZnCl_2$

Parameters	BP
Sc	0.0101
D_m ($m^2\ s^{-1}$)	9.97×10^{-5}
D_k ($m^2\ s^{-1}$)	4.37×10^{-7}
D_p ($m^2\ s^{-1}$)	3.38×10^{-7}
K_i (s^{-1})	1.48×10^{8}
IP_1 ($mmol \cdot g^{-1}$)	3.87×10^{-5}
IP_2 ($L \cdot mol^{-1}$)	1.81×10^{4}

experimental solution volume of 50×10^{-6} m^3. The bed dimensions—16 mm in height (H_b) and an average diameter of 8 mm—were selected to match the configuration used by Juela.[25]

The computational results were used to confirm the experimental conditions adopted in this study, namely the values in Table 4, which present the fixed variables and system properties used in the adsorption-column simulation. BP concentrations were intentionally selected based on experimental data.

The additional parameters required for the simulation were obtained by solving Eqns (S25–S32) and are summarized in Table 3. The adsorption column was designed with a bed height (*H*_b) of 0.001 m,[64] and the column diameter was defined according to the empirical ratio $H_b \cdot D = 10$.[65]

The Reynolds number (*Re*) calculated for each configuration was approximately 0.01, indicating that increased bed height reduces the interstitial fluid velocity. Moreover, a taller column height may lead to a greater pressure drop. On the other hand, shorter columns exhibited higher axial dispersion coefficients (*Dz*), with values of $5.82 \cdot 10^{-7}$ and $1.47 \cdot 10^{-7}$ $m^2 \cdot s^{-1}$ for H_b values of 0.001 m, respectively. The intraparticle diffusion coefficient (K_i) and molecular diffusivity in water (*Dp*) used in the simulations were 2.7×10^{-3} [46] and 5.1×10^{-11} $m^2 \cdot s^{-1}$,[66] respectively.

The computational simulation was designed to validate the adsorption performance observed in experiments, using the same parameters and conditions detailed in Table 2. In the simulation, the BP outlet concentration was set to 0 $\mu g \cdot L^{-1}$, corresponding to a theoretical removal efficiency (*ER%*) of 100%.

Simulation parameters included:

- Initial BP concentration: 30 $\mu g \cdot L^{-1}$ in water.
- Adsorbent concentration: 5 $g \cdot L^{-1}$ $ACZnCl_2$.
- System type: Batch (very low flow rate).

Figure S1 illustrates the process flowchart from Aspen Adsorption®, showing the simulated adsorption of BP onto $ACZnCl_2$. The D_Z was calculated using Eqn (S32). The *Re*. Given the low contaminant concentration and system flow rate (1.57×10^{-7} $m^3 \cdot s^{-1}$, with a cross-sectional area of 0.038 m^2), *Re* was found to be 4.12×10^{-3}, indicating laminar flow. Inputting these values yielded $D_Z = 3.47 \times 10^{-12}$ $m^2 \cdot s^{-1}$, confirming that axial dispersion was minimal and supporting the use of batch system assumptions.

The K_i used in the model, representing the resistance to mass transfer between $ACZnCl_2$ and BP, was calculated using Eqn (S18). Simulation outputs, along with sensitivity and optimization analyses, are summarized in Table 2. Concentrations were converted from $\mu g \cdot L^{-1}$ to $kmol \cdot m^{-3}$. Experimental measurements provided the bed diameter, porosity, and apparent density.[64]

The simulated process yielded a final BP concentration of 2.43×10^{-13} $kmol \cdot m^{-3}$ and a mixing fraction coefficient near zero, leading to a calculated *ER%* close to 100% Eqn (S1). This value was higher than those obtained experimentally.

The Aspen Adsorption® model showed that $ACZnCl_2$ was not fully saturated under these conditions. The higher simulated *ER%* is likely due to simplified assumptions, possible model over-idealization, or differences in calculation parameters. Additionally, factors such as low pollutant concentration and its impact on mass transfer dynamics may contribute to discrepancies between simulated and experimental data.[25] Further research is needed, as real adsorption behavior can depend on factors beyond the scope of the current simulation model.

For context, while there are no prior studies directly correlating BP adsorption onto $ACZnCl_2$, related research has explored BP removal using functional materials such as benzoic acid and magnetic cellulose. Correa-Navarro *et al.*[3] achieved a Q_t of 12 $\mu g \cdot g^{-1}$, with best fits to PFO and PSO kinetic models and the Langmuir isotherm. Atheba *et al.*[15] reported near-complete BP removal with AC from coconut residue, best described by the Temkin kinetic model and both the Langmuir and Freundlich isotherms, indicating favorable mono- and multilayer adsorption. Computational simulations help identify gaps in removal efficiency and guide optimization to achieve higher *ER%* in experimental systems.

Table 5 also presents the calculated parameters for all parabens evaluated in this study. It was observed that as the alkyl chain length of the parabens increases, the associated transport and adsorption parameters also increase. The H_b had no significant effect on the equilibrium or kinetic constants. Lastly, the Langmuir isotherm parameters (*IP1* and *IP2*), derived from Eqns (S20-S21), are also included in Table 5. The initial simulation aimed to assess the influence of column height on contaminant breakthrough concentration. Results demonstrated that H_b directly influences the outlet concentration of the treated effluent. Based on the data in Table 4, Aspen Adsorption® was inserted into the treatment model analyzed (Fig. 3).

© 2026 The Author(s).

Journal of Chemical Technology and Biotechnology published by John Wiley & Sons Ltd on behalf of Society of Chemical Industry (SCI).

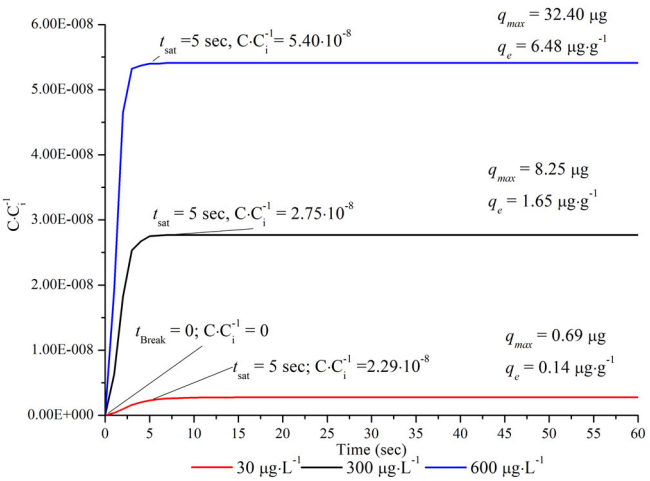


Figure 3. Simulation of the t_{break} and t_{sat} on a fixed bed.

This type of treatment is intended to be implemented downstream of conventional water and wastewater treatment processes, as parabens (BPs) can react with other ions and reagents present in water or effluents during earlier treatment stages, forming transformation products that may be more persistent or toxic than the parent compounds. One such transformation involves halogenation, which may occur through reactions with residual chlorine (Cl_2) during disinfection processes. These reactions typically target the phenolic moiety of parabens, forming mono- and dichlorinated derivatives, such as 3-chloro- and 3,5-dichloro-parabens. The reaction rates depend on factors such as pH, temperature, and the concentration of ammonium ions (NH_4^+).[67,68]

Another potential transformation route involves oxidation with ozone (O_3). Although undissociated parabens react slowly with pure ozone (rate constant ~10^5 $M^{-1}\cdot s^{-1}$), under alkaline conditions, O_3 decomposes to form hydroxyl radicals (•OH), which exhibit much higher reactivity (~10^9 $M^{-1}\cdot s^{-1}$).[69]

Based on the simulation data entered into the software, Fig. 3 presents the time-dependent behavior of paraben adsorption using $ACZnCl_2$ as the adsorbent, with initial concentrations of 30, 300, and 600 µg·L^{-1} and a fixed bed height of 0.001 m. When analyzing each paraben individually, a consistent trend emerged: the breakthrough time (t_{Break}) remained approximately constant across all initial concentrations. In adsorption systems, the most rapid adsorption typically occurs within the interior of the adsorbent's pores, driven by intraparticle diffusion and the adsorbate concentration gradient.[9] In this study, the adsorption–desorption dynamics are phenomenologically linked to the initial adsorbate concentration (C_i) through a first-order kinetic model, in which higher concentrations generally result in faster occupation of active adsorption sites.[8,11]

Another key feature visible in Fig. 3 is the mass transfer zone (MTZ), defined as the interval between breakthrough (t_{Break}) and saturation (t_{Sat}). This zone remained similar across all three tested concentrations. The observed exponential expansion of the MTZ is attributed to the progressive saturation of the $ACZnCl_2$ micropores in this region.[8,11,22]

The saturation time (t_{sat}) was also similar across concentrations, due to the relatively low paraben mass compared to the water volume. After this point, adsorption–desorption equilibrium prevails, characterized by a slower molecular diffusion step from the aqueous phase to the adsorbent surface, which continues until the adsorbent becomes fully saturated, signaling the need for regeneration or replacement.[9] Figure 3 presents the performance metrics and comparative calculations for the adsorption columns evaluated in this study.

Based on Fig. 3, the breakthrough time (t_{Break}) and saturation time (t_{sat}) were analyzed for the different concentrations. Equations (S22–S24) were applied using an adsorbent concentration of 5 g·L^{-1} and a flow rate of 5·10^{-7} m^3·s^{-1} to calculate the unknown parameters presented in Table 4. All time units were converted to seconds. For all BP concentrations tested, variation in BP concentration did not affect the transition zone.[25,64] It is also observed that lower inlet concentrations resulted in lower maximum adsorption Q_{MAX}. This result is explained by the fact that higher concentrations initiate adsorption more quickly due to the greater driving force.[8,11]

From a process design perspective, the 600 µg·L^{-1} concentration provides the highest adsorption capacity, ensuring that the adsorption step does not become a limiting factor in large-scale water or wastewater treatment processes. Although no simulation studies involving paraben adsorption have been published, similar behaviors have been reported in adsorption modeling studies for other organic pollutants.[21,25] Overall, the configuration using an inlet concentration of 600 µg·L^{-1} yielded the highest Q_{MAX} and Q_e values among the systems evaluated.

When these results are compared with bench-scale experiments, the simulated flow rate increased by an order of magnitude, shifting the hydrodynamic regime from laminar to turbulent. This transition explains the similarity observed in the concentration profiles along the bed, as turbulent flow reduces the influence of molecular diffusion.[70] The maintenance of x_{out} may also be related to the flow rate, since the software accounts for reversibility of the outlet stream, which in this case was limited to the water phase. Under turbulent conditions, the system rapidly transports BP through the fixed-bed column, preventing desorption from the $ACZnCl_2$ surface.

The $H_b \cdot D_B^{-1}$ ratio is another parameter that may have influenced the system behavior. The short interval between t_{sat} and t_{break} (0–5 s) suggests the presence of unsaturated pores within the $ACZnCl_2$ structure, indicating that this ratio can affect adsorption performance.[8,11,22]

Saturation time reflects the maximum adsorption capacity and the point at which active sites become fully occupied. Beyond this stage, adsorption and desorption reach a dynamic equilibrium governed by slower molecular diffusion from the aqueous phase to the adsorbent surface. This marks the onset of conditions that would eventually require adsorbent regeneration or replacement.[9]

To date, no adsorption studies have reported BP removal using $ACZnCl_2$ at environmentally relevant concentrations. Table 6 summarizes existing BP adsorption systems using other functional materials. Based on the data in Table 5 and the results of this study, a technical comparison highlights the scientific relevance of our findings. Although the removal efficiency (77.6%) appears numerically lower than some values reported in Table 5, this study evaluates BP at 30 µg·L^{-1} (0.03 mg·L^{-1}), whereas most literature values fall within 10–200 mg·L^{-1}. Even the graphene oxide study, which uses the lowest concentration in the Table (0.06 mg·L^{-1}), still operates at a concentration 20 times higher than the one tested here.

Removing contaminants at trace levels is inherently more challenging due to the minimal driving force for adsorption.[28]

 © 2026 The Author(s).
Journal of Chemical Technology and Biotechnology published by John Wiley & Sons Ltd on behalf of Society of Chemical Industry (SCI).

Table 6. Data from experimental and computational studies using different adsorbents for BP removal

Adsorbent	A^a($g{\cdot}L^{-1}$)	C^b($mg{\cdot}L^{-1}$)	*ER%*	E^C or $C^{Reference}$
Coconut biochar-based activated carbon	4	100	97	E[15]
AC *Elaeis guineensis*	2	10–100	99	E[14]
Modified Cellulose with Succinate Groups	2	10–100	90	E[3]
Graphene Oxide	5	0.6	84.3	E[71]
Metal organic frameworks (MOFs)	0.4	10	98	E[72]
Oak Bark Activated Carbon	1	20–200	98	E[73]
Biochar from Fiche Bagasse	2	10–60	90	E[74]
$ACZnCl_2$	5	50–100	99	C[75]

A^a = Adsorbent; C^b = Concentration of BP; E^C or C = Experimental or Computational.

Demonstrating 77.6% removal at $\mu g{\cdot}L^{-1}$ concentrations therefore indicates a strong chemical affinity between BP and $ACZnCl_2$—greater than that of materials that require much higher pollutant loads (typically grams) to perform effectively. Additionally, this study used an adsorbent dosage of 5 $g{\cdot}L^{-1}$, the same as graphene oxide and $ACZnCl_2$ in the literature. Materials such as *Elaeis guineensis* AC or oak bark achieve 98–99% removal, but only in highly concentrated (20–100 $mg{\cdot}L^{-1}$) solutions. By contrast, this study reflects environmental reality, as parabens typically occur in rivers and effluents at $\mu g{\cdot}L^{-1}$ levels, making the results more applicable to real water-polishing scenarios.

Removing contaminants at trace levels is inherently more challenging due to the minimal driving force for adsorption.[28] Demonstrating 77.6% removal at $\mu g{\cdot}L^{-1}$ concentrations therefore indicates a strong chemical affinity between BP and $ACZnCl_2$—greater than that of materials that require much higher pollutant loads (typically grams) to perform effectively. Additionally, this study used an adsorbent dosage of 5 $g{\cdot}L^{-1}$, the same as graphene oxide and $ACZnCl_2$ in the literature. Materials such as *Elaeis guineensis* AC or oak bark achieve 98–99% removal, but only in highly concentrated (20–100 $mg{\cdot}L^{-1}$) solutions. By contrast, this study reflects environmental reality, as parabens typically occur in rivers and effluents at $\mu g{\cdot}L^{-1}$ levels, making the results more applicable to real water-polishing scenarios.

This study aligns with the few works in Table 6 that combine experimental and computational approaches. The simulation results obtained with $ACZnCl_2$ at much lower BP concentrations indicate that, under ideal contact conditions and without external interference, the material exhibits a theoretical saturation capacity of 100%. The difference between the theoretical (100%) and experimental (77.6%) removal efficiencies provides valuable insight into mass-transfer limitations that may be overlooked in studies conducted at high pollutant concentrations.

The primary strength of this work lies in its methodological novelty and environmental relevance. Unlike most studies that focus on high pollutant concentrations (10–200 $mg{\cdot}L^{-1}$), this research demonstrates that $ACZnCl_2$ is effective at trace levels (30 $\mu g{\cdot}L^{-1}$), which better represent micropollutant conditions in natural waters. Integrating experimental data with Aspen Adsorption® simulations also provides a scalable predictive tool for the pharmaceutical and water-treatment sectors, addressing a gap in the literature regarding computational modeling of paraben removal. However, some limitations must be acknowledged. The current simulation assumes an isothermal, single-component system. In real wastewater, competing ions, and natural organic matter may alter mass-transfer dynamics and reduce adsorption capacity. Furthermore, the discrepancy between theoretical (100%) and experimental (77.6%) removal suggests that internal diffusion resistances and model idealizations require further refinement.

While this study establishes the technical feasibility of using $ACZnCl_2$ for trace-level BP removal, several research avenues remain. Future work should evaluate adsorption performance in real environmental samples, where natural organic matter and inorganic ions may compete for active sites and influence breakthrough behavior. To advance toward industrial application, pilot-scale studies should incorporate non-isothermal conditions, pressure-drop effects in taller columns, and realistic hydraulic loads. Investigating the removal of paraben transformation products—such as chlorinated or oxidized derivatives formed during secondary treatment—would also provide a more comprehensive assessment of $ACZnCl_2$ as a water-polishing material. Finally, a life-cycle assessment and economic analysis are needed to confirm the long-term sustainability and cost-effectiveness of this waste-derived adsorbent relative to commercial activated carbons.

CONCLUSIONS

This study demonstrates that activated carbon produced from spent coffee grounds and activated with $ZnCl_2$ ($ACZnCl_2$) is an effective, reusable, and sustainable adsorbent for the removal of butylparaben (BP) from aqueous solutions. The material achieved its highest removal efficiency (77.6 ± 0.4%) at the lowest tested concentration (30 $\mu g{\cdot}L^{-1}$), highlighting its strong affinity for BP at environmentally relevant micropollutant levels.

Kinetic analysis revealed that BP adsorption onto $ACZnCl_2$ follows both PFO and PSO models, reaching equilibrium within approximately 100 min. Equilibrium data were best described by the Langmuir isotherm, suggesting monolayer adsorption on a homogeneous surface and confirming the structural uniformity of the prepared activated carbon.

Thermodynamic evaluation revealed that the adsorption process is spontaneous ($\Delta G \leq 0$) and exothermic ($\Delta H \leq 0$). Variations in salt concentration primarily affected electrostatic interactions but did not significantly reduce adsorption capacity, supporting the applicability of $ACZnCl_2$ in real water matrices. The adsorbent also maintained high performance over at least six reuse cycles, and post-treatment *Allium cepa* assays confirmed the reduction of cytotoxic and genotoxic effects, demonstrating improved effluent safety.

 © 2026 The Author(s).
Journal of Chemical Technology and Biotechnology published by John Wiley & Sons Ltd on behalf of Society of Chemical Industry (SCI).

Based on the optimized simulation results, the designed adsorption column is suitable for small-scale domestic applications. For water containing 600 $\mu g \cdot L^{-1}$ of parabens, the recommended configuration includes a height-to-diameter ratio ($Hb \cdot D^{-1}$) of 10, a bed height of 0.001 m, and $ACZnCl_2$ particle diameters of 1.69×10^{-7} m. The system operates at an inlet flow rate of 5×10^{-7} $m^3 \cdot s^{-1}$ and can supply treated water continuously, requiring full bed replacement once per day as saturation approaches a breakthrough ratio (C/C_i) of 0.999.

Importantly, this work addresses a critical gap in the literature: while most adsorption studies evaluate BP removal at $mg \cdot L^{-1}$ concentrations, this study demonstrates high efficiency at $\mu g \cdot L^{-1}$ levels, which more accurately reflect environmental conditions. Removing contaminants at trace concentrations is inherently challenging due to the low driving force for adsorption; thus, achieving 77.6% removal at 30 $\mu g \cdot L^{-1}$ underscores the strong chemical affinity between BP and $ACZnCl_2$. The use of spent coffee grounds as a precursor further advances circular-economy principles by converting an abundant waste material into a high-value adsorbent.

Overall, these findings establish $ACZnCl_2$ derived from spent coffee grounds as a promising, sustainable, and scalable material for BP removal. Its high efficiency at environmentally relevant concentrations, reusability, favorable thermodynamic behavior, and validated performance through simulation highlight its potential for environmentally relevant water-treatment applications.

ACKNOWLEDGEMENTS

We would like to thank the multi-user laboratories of UTFPR, especially LabMult in Londrina, Lama in Apucarana and CAMulti in Campo Mourão, all in the state of Paraná, Brazil.

ChatGPT 4.0 (OpenAI), and Gemini were used to refine the language and improve the readability of certain sections of this manuscript. All AI-generated text was reviewed and edited by the authors for accuracy and style. The Article Processing Charge for the publication of this research was funded by the Coordenação de Aperfeiçoamento de Pessoal de Nível Superior - Brasil (CAPES) (ROR identifier: 00x0ma614).

DATA AVAILABILITY STATEMENT

Upon reasonable request from the corresponding author.

CONFLICT OF INTEREST

No potential conflict of interest was reported by the authors.

SUPPORTING INFORMATION

Supporting information may be found in the online version of this article.

REFERENCES

1 Xiang J, Lv BR, Y-j S, Chen W-m and Zhang J-l, Environmental pollution of paraben needs attention: a study of methylparaben and butylparaben co-exposure trigger neurobehavioral toxicity in zebrafish. *Environ Pollut* **356**:124370 (2024).
2 Vale F, Sousa CA, Sousa H, Santos L and Simões M, Impact of parabens on microalgae bioremediation of wastewaters: a mechanistic study. *Chem Eng J* **442**:136374 (2022).
3 Correa-Navarro YM, Rivera-Giraldo JD and Cardona-Castaño JA, Modified cellulose for adsorption of Methylparaben and Butylparaben from an aqueous solution. *ACS Omega* **9**:30224–30233 (2024).
4 Maske P, Dighe V, Mote C and Vanage G, n-Butylparaben exposure through gestation and lactation impairs spermatogenesis and steroidogenesis causing reduced fertility in the F1 generation male rats. *Environ Pollut* **256**:112957 (2020).
5 Li Z, Jia K, Chen X, Guo J, Zheng Z, Chen W *et al*., Exposure to Butylparaben induces craniofacial bone developmental toxicity in zebrafish (*Danio rerio*) embryos. *Ecotoxicol Environ Saf* **265**:115523 (2023).
6 Huang L, Xu J, Jia K, Wu Y, Yuan W, Liao Z *et al*., Butylparaben induced zebrafish (*Danio rerio*) kidney injury by down-regulating the PI3K-AKT pathway. *J Hazard Mater* **470**:134129 (2024).
7 Medkova D, Hollerova A, Riesova B, Blahova J, Hodkovicova N, Marsalek P *et al*., Pesticides and parabens contaminating aquatic environment: acute and sub-chronic toxicity towards early-life stages of freshwater fish and amphibians. *Toxics* **11**:11040333 (2023).
8 da S RBC, de MLEZ, Santo DE, Peron AP, de SDC, Bona E *et al*., Removal of bentazone using activated carbon from spent coffee grounds. *J Chem Technol Biotechnol* **99**:1342–1355 (2024).
9 do NRF, de LACA, Vidal CB, de Q MD and Raulino GSC, *Adsorção: aspectos teóricos e aplicações ambientais*. Imprensa Univ, Fortaleza, p. 308 (2020).
10 FBT R and da Silva WL, Biosorption: a review of promising alternative methods in wastewater treatment. *Rev Mater* **27**:1312 (2022).
11 da RSAF, da S RBC, de MLEZ, JMP V, Scapin D, Santo DE *et al*., Evaluation and simulation of the adsorption capacity of Octocrylene sunscreen on commercial carbon and biochar from spent coffee beans. *Processes* **12**:12061249 (2024).
12 Wei Y, Liu X, Wang Z, Chi Y, Yue T, Dai Y *et al*., Adsorption and catalytic degradation of preservative parabens by graphene-family nanomaterials. *Sci Total Environ* **806**:150520 (2022).
13 Wang T, Zhai Y, Zhu Y, Li C and Zeng G, A review of the hydrothermal carbonization of biomass waste for hydrochar formation: process conditions, fundamentals, and physicochemical properties. *Renew Sustain Energy Rev* **90**:223–247 (2018).
14 Moreno-Marenco AR, Giraldo L and Moreno-Piraján JC, Adsorption of n-butylparaben from aqueous solution on surface of modified granular activated carbons prepared from African palm shell. Thermodynamic study of interactions. *J Environ Chem Eng* **8**:103969 (2020).
15 Atheba P, Allou NB, Drogui P and Trokourey A, Adsorption kinetics and thermodynamics study of Butylparaben on activated carbon coconut based. *J Encapsulation Adsorpt Sci* **8**:39–57 (2018).
16 Ayala J and Fernández B, Treatment of mining waste leachate by the adsorption process using spent coffee grounds. *Environ Technol* **40**:2037–2051 (2019).
17 Javier Sánchez A, Characterization of activated carbon produced from coffee residues by chemical and physical activation. *KTH Chem Sci Eng* **66**:06 (2011).
18 Jagdale P, Ziegler D, Rovere M, Tulliani JM and Tagliaferro A, Waste coffee ground biochar: a material for humidity sensors. *Sensors (Switzerland)* **19**:19040801 (2019).
19 Yasir HA, Zein SH, Holliday MC, Jabbar KJ, Ahmed U and Jalil AA, Comparison of activated carbon and low-cost adsorbents for removal of 2,4-dichlorophenol from wastewater using Aspen adsorption and response surface methodology. *Environ Technol* **45**:3029–3047 (2024).
20 Mirzaeifard Z and Shariatinia Z, Economical, one-pot, and green synthesis of plant-based carbon quantum dots for efficient visible-light photocatalytic dye degradation and water purification. *J Taiwan Inst Chem Eng* **163**:105655 (2024).
21 Soriano AN, Orfiana ON, Pangon MBJ, Nieva AD and Adornado AP, Simulated biosorption of Cd(II) and Cu(II) in single and binary metal systems by water hyacinth (*Eichhornia crassipes*) using aspen adsorption®. *ASEAN J Chem Eng* **16**:21–43 (2016).
22 de Moraes LEZ, Marcoti FAO, Lucio MAN, Rocha BC d S, Rocha LB, Romero AL *et al*., Analysis and simulation of adsorption efficiency of herbicides Diuron and Linuron on activated carbon from spent coffee beans. *Processes* **12**:9 (2024).
23 Custodio RF, Junior OV, Vieira AL, de Souza TL, Bezerra FL d A and Bonfim-Rocha L, Techno-economic and CO_2 net assessment of dimethyl carbonate production from biomass-derived methanol. *Processes* **13**:13020573 (2025).
24 Yousef R, Qiblawey H and El-Naas MH, Evaluation of activated carbon fiber packed-bed for the treatment of gas-to-liquid wastewater:

 © 2026 The Author(s).
Journal of Chemical Technology and Biotechnology published by John Wiley & Sons Ltd on behalf of Society of Chemical Industry (SCI).

experimental, modeling and ASPEN adsorption simulation. *Emergent Mater* **8**:1591–1603 (2024).
25 Juela DM, Comparison of the adsorption capacity of acetaminophen on sugarcane bagasse and corn cob by dynamic simulation. *Sustain Environ Res* **30**:1 (2020).
26 Debien ICN, Vardanega R, Santos DT and Meireles MAA, Pressurized liquid extraction as a promising and economically feasible technique for obtaining Beta-ecdysone-rich extracts from Brazilian ginseng (*Pfaffia glomerata*) roots. *Sep Sci Technol* **50**:1647–1657 (2015).
27 Dean JR, Pressurized liquid extraction. *Extr Tech Environ Anal* **10**:171–204 (2022).
28 Ersan G, Apul OG, Perreault F and Karanfil T, Adsorption of organic contaminants by graphene nanosheets: a review. *Water Res* **126**:385–398 (2017).
29 Gonçalves Júnior DR, de Araújo PCC, Simões ALG, Voll FAP, Parizi MPS, de Oliveira LH *et al*., Assessment of the adsorption capacity of phenol on magnetic activated carbon. *Asia-Pac J Chem Eng* **17**:1 (2022).
30 Spaltro A, Simonetti S, Torrellas SA, Rodriguez JG, Ruiz D, Juan A *et al*., Adsorption of bentazon on CAT and CARBOPAL activated carbon: experimental and computational study. *Appl Surf Sci* **433**:487–501 (2018).
31 Milanković V, Tasić T, Pejčić M, Pašti I and Lazarević-Pašti T, Spent coffee grounds as an adsorbent for malathion and Chlorpyrifos—kinetics, thermodynamics, and eco-neurotoxicity. *Foods* **12**:12122397 (2023).
32 Zbair M, El Hadrami A, Bellarbi A, Monkade M, Zradba A and Brahmi R, Herbicide diuron removal from aqueous solution by bottom ash: kinetics, isotherm, and thermodynamic adsorption studies. *J Environ Chem Eng* **8**:103667 (2020).
33 Fiskesjö G, The allium test as a standard in environmental monitoring. *Hereditas* **102**:99–112 (1985).
34 Rasyid NQ and Muawanah R, *Konsentrasi Pengawet Paraben pada Produk Perawatan Tubuh*, Seminar Nasional Hasil Penelitian & Pengabdian Kepada Masyarakat (SNP2M), pp. 83–86 (2017).
35 Amin FR, Huang Y, He Y, Zhang R, Liu G and Chen C, Biochar applications and modern techniques for characterization. *Clean Technol Environ Policy* **18**:1457–1473 (2016).
36 Huang Q, Song S, Chen Z, Hu B, Chen J and Wang X, Biochar-based materials and their applications in removal of organic contaminants from wastewater: state-of-the-art review. *Biochar* **1**:45–73 (2019).
37 Boehm HP, Surface oxides on carbon and their analysis: a critical assessment. *Carbon N Y* **40**:145–149 (2002).
38 Anisuzzaman SM, Joseph CG, Krishnaiah D, Bono A, Suali E, Abang S *et al*., Removal of chlorinated phenol from aqueous media by guava seed (*Psidium guajava*) tailored activated carbon. *Water Resour Ind* **16**:29–36 (2016).
39 Heidarinejad Z, Dehghani MH, Heidari M, Javedan G, Ali I and Sillanpää M, Methods for preparation and activation of activated carbon: a review. *Environ Chem Lett* **18**:393–415 (2020).
40 Giannakopoulos S, Frontistis Z, Vakros J, Poulopoulos SG, Manariotis ID and Mantzavinos D, Combined activation of persulfate by biochars and artificial light for the degradation of sulfamethoxazole in aqueous matrices. *J Taiwan Inst Chem Eng* **136**:104440 (2022).
41 Grilla E, Vakros J, Konstantinou I, Manariotis ID and Mantzavinos D, Activation of persulfate by biochar from spent malt rootlets for the degradation of trimethoprim in the presence of inorganic ions. *J Chem Technol Biotechnol* **95**:2348–2358 (2020).
42 Liu Y and Shen L, From Langmuir kinetics to first- and second-order rate equations for adsorption. *Langmuir* **24**:11625–11630 (2008).
43 Benaouda B, Iman G and Michalkiewicz B, Study on anionic dye toxicity reduction from simulated media by MnO_2/agro-biomass based-AC composite adsorbent. *Ind Crop Prod* **208**:117789 (2024).
44 Edet UA and Ifelebuegu AO, Kinetics, isotherms, and thermodynamic modeling of the adsorption of phosphates from model wastewater using recycled brick waste. *Processes* **8**:6 (2020).
45 Sen Gupta S and Bhattacharyya KG, Kinetics of adsorption of metal ions on inorganic materials: a review. *Adv Colloid Interface Sci* **162**:39–58 (2011).
46 Inglezakis VJ, Balsamo M and Montagnaro F, Liquid-solid mass transfer in adsorption systems - an overlooked resistance? *Ind Eng Chem Res* **59**:22007–22016 (2020).
47 Stephen B, Paul E and Edward T, Adsorption of gases in multimolecular layers. *J Am Chem Soc* **407**:309–319 (1936).
48 Do DD, Adsorption analysis: equilibria and kinetics. *Chem Eng* **2**:913 (1998).
49 Milanković V, Tasić T, Brković S, Potkonjak N, Unterweger C, Bajuk-Bogdanović D *et al*., Spent coffee grounds-derived carbon material as an effective adsorbent for removing multiple contaminants from wastewater: a comprehensive kinetic, isotherm, and thermodynamic study. *J Water Process Eng* **63**:105507 (2024).
50 Singh NB, Nagpal G, Agrawal S and Rachna, Water purification by using adsorbents: a review. *Environ Technol Innov* **11**:187–240 (2018).
51 Dubinin MM, The equation of the characteristic curve of activated charcoal. *Proc USSR Acad Sci* **55**:327–329 (1947).
52 Kunin R and Gustafson RL, Ion Exchange. *Anal Chem* **40**:136–138 (1968).
53 Karri RR, Sahu JN and Jayakumar NS, Optimal isotherm parameters for phenol adsorption from aqueous solutions onto coconut shell based activated carbon: error analysis of linear and non-linear methods. *J Taiwan Inst Chem Eng* **80**:472–487 (2017).
54 Siregar CA and Siregar AM, Rancang Bangun Mesin Giling Kopi Untuk Menunjang dan Membuka Unit Usaha Baru Mitra Deli Coffe. *ABDI SABHA (Jurnal Pengabdian kepada Masyarakat)* **3**:174–180 (2022).
55 Saberian M, Li J, Donnoli A, Bonderenko E, Oliva P, Gill B *et al*., Recycling of spent coffee grounds in construction materials: a review. *J Clean Prod* **289**:125837 (2021).
56 Wang SY, Bowman L and Ding M, Methyl jasmonate enhances antioxidant activity and flavonoid content in blackberries (*Rubus sp*.) and promotes antiproliferation of human cancer cells. *Food Chem* **107**:1261–1269 (2008).
57 Sadasivam S, Krishna SK, Ponnusamy K, Nagarajan GS, Kang TW and Venkatesalu SC, Equilibrium and thermodynamic studies on the adsorption of an organophosphorous pesticide onto "waste" jute fiber carbon. *J Chem Eng Data* **55**:5658–5662 (2010).
58 Santo DE, Dusman E, da Silva Gonzalez R, Romero AL, dos Santos Gonçalves do Nascimento GC, de Souza Moura MA *et al*., Prospecting toxicity of octocrylene in *Allium cepa L*. and *Eisenia fetida Sav*. *Environ Sci Pollut Res* **30**:8257–8268 (2023).
59 Todorovac E, Durmisevic I, Cajo S, Haverić A and Mesic A, Evaluation of DNA and cellular damage caused by methyl-, ethyl- and butylparaben *in vitro*. *Toxicol Environ Chem* **103**:85–103 (2021).
60 Güzel Bayülken D and Ayaz Tüylü B, *In vitro* genotoxic and cytotoxic effects of some paraben esters on human peripheral lymphocytes. *Drug Chem Toxicol* **42**:386–393 (2019).
61 de Almeida EA, Pinto MEN, Maehashi AE, Rodrigues MAV, Galdino E d M, Santo DE *et al*., Genotoxic and Toxicopathological responses to Ethylparaben in plants: potential impacts to crop yields. *Toxics* **13**:11 (2025).
62 Namasivayam C and Sangeetha D, Removal and recovery of vanadium(V) by adsorption onto $ZnCl_2$ activated carbon: kinetics and isotherms. *Adsorption* **12**:103–117 (2006).
63 Dąbek L, Sorption of zinc ions from aqueous solutions on regenerated activated carbons. *J Hazard Mater* **101**:191–201 (2003).
64 Anisuzzaman SM, Bono A, Krishnaiah D and Tan YZ, A study on dynamic simulation of phenol adsorption in activated carbon packed bed column. *J King Saud Univ* **28**:47–55 (2016).
65 Lakshmipathy R and Sarada NC, A fixed bed column study for the removal of Pb^{2+} ions by watermelon rind. *Environ Sci Water Res Technol* **1**:244–250 (2015).
66 Biswas S, Sharma S, Mukherjee S, Meikap BC and Sen TK, Process modelling and optimization of a novel Semifluidized bed adsorption column operation for aqueous phase divalent heavy metal ions removal. *J Water Process Eng* **37**:101406 (2020).
67 Yoom H, Shin J, Ra J, Son H, Ryu D, Kim C *et al*., Transformation of methylparaben during water chlorination: effects of bromide and dissolved organic matter on reaction kinetics and transformation pathways. *Sci Total Environ* **634**:677–686 (2018).
68 Mao Q, Ji F, Wang W, Wang Q, Hu Z and Yuan S, Chlorination of parabens: reaction kinetics and transformation product identification. *Environ Sci Pollut Res* **23**:23081–23091 (2016).
69 López-Timoner R, Duarte-Alvarado V, Castillo MÁ, Santos-Juanes L, Arques A and Amat AM, Parabens and Methylisotiazolinone (MIT): preservatives with different behaviors when subjected to ozone and ultraviolet light treatments. *Water (Switzerland)* **15**:21 (2023).
70 Flynn HG, Transport phenomena. *Phys Today* **15**:96–98 (1962).
71 Tsubouchi LMS, de Ameida EA, Santo DE, Bona E, Pereira GLD, Jegatheesan V *et al*., *Water (Switzerland)* **16**:16243703 (2024).
72 Chen C, Xu L, Huo JB, Gupta K and Fu ML, *Chem Eng J* **391**:123552 (2020).
73 Paluch D, Wolski R, Bazan-Wozniak A and Pietrzak R, *Materials (Basel)* **18**:18132984 (2025).
74 Correa-Navarro YM, Rivera-Giraldo JD and Murcia-García JD, *Data Br* **57**:111113 (2024).
75 Martins WM, DosSantos AR, Tractz GT, Bonfim-Rocha L, Peron AP and Junior OV, *Processes* **13**:13082481 (2025).

© 2026 The Author(s).
Journal of Chemical Technology and Biotechnology published by John Wiley & Sons Ltd on behalf of Society of Chemical Industry (SCI).